Adsorption (2014) 20:843–853
DOI 10.1007/s10450-014-9626-8

Evaluation of approximations for concentration-dependent micropore diffusion in sorbent with bidisperse pore structure

Guanghua Ye · Xuezhi Duan · Zhijun Sui · Kake Zhu · Xinggui Zhou · Weikang Yuan

Received: 1 April 2014 / Revised: 16 June 2014 / Accepted: 23 June 2014 / Published online: 9 July 2014

Abstract Average diffusivity linear driving force (AD-LDF) and concentration-dependent diffusivity linear driving force (CDD-LDF) approximations are introduced to simplify the precise model describing the concentration-dependent micropore diffusion in bidisperse sorbents, and are compared with the precise model in predicting the dynamics of a sorption process under two different perturbations (i.e., step change perturbations and sinusoidal wave perturbation) with different concentrations imposed at the exterior surface of the bidisperse sorbent. The performance of the two approximations is validated by the precise model and experiments. The AD-LDF performs better in step adsorption and CDD-LDF does better in step desorption. Under sinusoidal wave perturbation, the CDD-LDF performs better. The different levels of consistency of the two approximations with the precise model are attributed to the different definitions of the diffusivities.

Keywords Approximation · Linear driving force · Concentration-dependent · Micropore diffusion · Bidisperse

List of symbols

b	Langmuirian gas–solid interaction parameter (m^3/mol)
C	Concentration in macropores (mol/m^3)
C_b	Concentration in bulk fluid (mol/m^3)
C_h	Upper limit concentration in bulk fluid (mol/m^3)
C_i	Initial concentration in macropores (mol/m^3)
D	Diffusivity in Glueckauf's LDF (m^2/s)
D_c	Diffusivity for micropore diffusion (m^2/s)
D_{c0}	Limiting micropore diffusivity at zero loading in crystals (m^2/s)
$\overline{D_c}$	Average diffusivity for micropore diffusion (m^2/s)
D_{eff}	Effective diffusivity (m^2/s)
D_p	Diffusivity for macropore diffusion (m^2/s)
q	Loading in crystals (mol/m^3)
q_i	Initial loading in crystals (mol/m^3)
q_s	Saturation loading in crystals (mol/m^3)
q^*	Equilibration loading in crystals (mol/m^3)
$\overline{q}$	Volume-averaged loading in crystals (mol/m^3)
q_{max}	Maximum loading in crystals (mol/m^3)
r	Crystal coordinate (m)
r_c	Radius of crystal (m)
R	Sorbent coordinate (m)
R_p	Radius of sorbent (m)
t	Time (s)
Δt_a	Adsorption time (s)
Δt_d	Desorption time (s)
ΔT_a	Perturbation period for adsorption (s)
ΔT_d	Perturbation period for desorption (s)

Greek letters

ε	Porosity of sorbent, dimensionless
ρ	Density of sorbent (kg/m^3)
θ	Dimensionless adsorbed amount of adsorbate
Φ	Dimensionless absolute deviation

Subscripts and superscripts

a	Adsorption
b	Bulk
c	Crystal
d	Desorption
h	High value

G. Ye · X. Duan · Z. Sui · K. Zhu · X. Zhou (✉) · W. Yuan
State Key Laboratory of Chemical Engineering, East China University of Science and Technology, Shanghai 200237, China
e-mail: xgzhou@ecust.edu.cn

i	Initial
p	Pellet
s	Saturation
0	Zero loading
*	Equilibration
Max	Maximum
AD-LDF	Average diffusivity linear driving force approximation
CDD-LDF	Concentration-dependent diffusivity linear driving force approximation
eff	Effective
precise	Precise bidisperse pore diffusion model

1 Introduction

Most industrial porous sorbents, especially granulated zeolites, have a bidisperse pore structure, consisting of the macropores between microparticles (e.g., crystals) and the micropores in the microparticles. There are two distinct diffusional resistances to mass transfer (i.e., the macropore diffusional resistance and the micropore diffusional resistance) in the bidisperse sorbents, and two film resistances on the surfaces of sorbents and microparticles (Do 1990), in which the four mass transfer resistances have their influences on the overall performance of adsorption in series or parallel.

Modeling the mass transfer process in the bidisperse sorbents is needed for industrial design and optimization of adsorption separation operations, e.g., pressure swing adsorption, temperature swing adsorption, and simulated moving bed absorption. To evaluate the relative importance of the diffusion resistances, a criterion provided by Ruthven and Loughlin (1972) can be used, which is based on a bidisperse porous model established by Ruckenstein et al. (1971) When the mass transfer is controlled by the macropore or micropore diffusion, the macropore or micropore diffusion degenerated models can be used. However, in most cases, both the resistances exist, and thus the bidisperse models have to be used to reflect the real nature of the bidisperse sorbents.

The precise bidisperse model is constructed by coupling the mass balance equations for the macropores with those for the micropores. Different diffusion mechanisms are involved in the pore network, including molecular diffusion, Knudsen diffusion, and surface diffusion. In micropores, a precise treatment of the driving force for diffusion is the chemical potential gradient (Farooq and Ruthven 1991; Farooq et al. 1993; Jolimaitre et al. 2002; Khalighi et al. 2012; Lettat et al. 2011). All this makes the precise bidisperse model very complicated. Solving these equations without any simplification is time consuming (Cruz et al. 2006). To match the fast dynamics of the adsorption process for real time simulation, control and optimization, approximations with acceptable accuracy are generally required.

The most widely used approximation for the mass transfer in micropores or macropores with the assumption of the constant Fick's diffusivity is the linear driving force (LDF) (Glueckauf and Coates 1947), i.e.,

$$\frac{\partial \overline{q}}{\partial \tau} = \frac{15D}{R_p^2}(q^* - \overline{q}) \tag{1}$$

where q^* is the loading on the surface and $\overline{q}$is the volume-average loading in the pellet. With this LDF approximation, the partial differential mass balance equation in the particle is transformed into a much simpler ordinary differential equation, in which the uptake rate is proportional to the difference between the surface concentration and the average concentration within the sorbents. The LDF can be derived by assuming a parabolic concentration profile (Liaw et al. 1979) which has been widely used to approximate the concentration profile in sorbents (Lai and Tan 1991; Do and Rice 1995; Yao and Tien 1993, 1998; Zhang and Ritter 1997; Xiu 1996; Xiu et al. 1997) and catalysts (Goto et al. 1990; Goto and Hirose 1993). Li and Yang (1999) proposed a generalized concentration profile and showed that only the 2nd-order and 5th-order binomial concentration profile could yield a proper volume-average uptake.

For the mass transfer in the bidisperse sorbents, Azevedo and Rodrigues (1999) proposed a bilinear driving force (bi-LDF) approximation with the assumption of the constant Fick's diffusivity for both micropore and macropore diffusion. The bi-LDF approximation can be used for the simulation of concentration-independent diffusion processes (Azevedo and Rodrigues 1999; Grande and Rodrigues 2004; Liu et al. 2012), but it is inadequate for the simulation of concentration-dependent diffusion processes (Krishna and Baur 2003).

The diffusivity could be measured by various experimental methods, e.g., zero-length column method, uptake rate measurements, chromatographic measurements etc., which is summarized in some works (Do 1998; Ruthven 2008; Ruthven et al. 2008). In fact, the Fick's diffusivity in micropores is strongly concentration-dependent, as is evidenced by the detailed experimental studies of diffusion in zeolites and carbon molecular sieves (Jolimaitre et al. 2001, 2002; Garg and Ruthven 1972; Skoulidas and Sholl 2001; Ruthven 2004; Jobic et al. 2005; Kärger and Ruthven 1992). Therefore, adequate approximations are needed to simplify the mass balance equations describing the concentration-dependent diffusion. Botte et al. (1999), Grande and Rodrigues (2005), as well as Khalighi et al. (2012) employed the concentration-dependent diffusivity in LDF equation to simplify the mass balance equations, in which

the models were however only used for the specific adsorption separation condition. Up to now, a systematic evaluation of different LDF based strategies for the simplification of concentration-dependent diffusion process has not been reported in the literature.

In this work, two approximations are introduced to simplify the micropore diffusion in the bidisperse sorbents, namely, the average diffusivity linear driving force (AD-LDF) approximation and the concentration-dependent diffusivity linear driving force (CDD-LDF) approximation. The two approximations are systematically evaluated under two different perturbations (i.e., step change perturbations and sinusoidal wave perturbation) with different concentrations imposed at the exterior surface of the bidisperse sorbent. These perturbations are frequently encountered in practical operations (Cruz et al. 2006). The concentration profile in the macropores, determined by the precise bidisperse model, is set as the boundary condition for micropore diffusion equations to reflect the real nature of bidisperse sorbents, and both the AD-LDF and CDD-LDF for micropore diffusion are subject to this same boundary condition. For different perturbations with different concentrations, appropriate approximations are suggested for the concentration-dependent diffusion under different conditions. Finally, comparison with experiments (Garg and Ruthven 1972; Ruthven 2004) and traditional LDF is made to validate the two approximations.

2 Theory

2.1 Models assumptions

It is assumed that the spherical sorbent consists of uniform microporous spheres and no temperature gradient exists in the sorbent (Solsvik and Jakobsen 2011; Hu and Do 1996). The following additional assumptions are made:

(1) Ideal gas and negligible viscous flow in the sorbent.
(2) No film resistances on the exterior surfaces of the sorbents and microparticles.
(3) Instantaneous equilibrium between the gas phase in the macropores and adsorbed phase on the surface of the microparticles.
(4) Negligible adsorption in the macropores and Langmuir adsorption in the micropores.
(5) The driving force for molecular transport assumed to be the chemical potential gradient and the mobility assumed to be concentration-independent.

2.2 Precise bidisperse pore diffusion model

The precise bidisperse pore diffusion model is used as the standard to evaluate the two approximations, and the concentration profile in macropores is set as the boundary condition for micropore diffusion equations to reflect the real nature of bidisperse sorbents.

The mass balance equation in macropores is

$$\varepsilon\frac{\partial C}{\partial t}+\rho\frac{\partial \overline{q}}{\partial t}=\varepsilon\frac{D_p}{R^2}\frac{\partial}{\partial R}\left(R^2\frac{\partial C}{\partial R}\right) \tag{2}$$

where $\overline{q}$ is the volume-average loading. The initial and boundary conditions are

$$\frac{\partial C}{\partial R}=0 \; at \; R=0,\; t>0 \tag{3}$$

$$C=C_b \; at \; R=R_p,\; t>0 \tag{4}$$

$$C=C_i \; at \; t=0,\; 0\le R\le R_p \tag{5}$$

where C_b is the bulk gas concentration at the exterior surface of the sorbent.

The mass balance equation in the micropore is

$$\frac{\partial q}{\partial t}=\frac{1}{r^2}\frac{\partial}{\partial r}\left(r^2D_c\frac{\partial q}{\partial r}\right) \tag{6}$$

and the initial and boundary conditions are

$$\frac{\partial q}{\partial r}=0 \; at \; r=0,\; t>0 \tag{7}$$

$$q=f(C) \; at \; r=r_c,\; t>0 \tag{8}$$

$$q=q_i \; at \; t=0,\; 0\le r\le r_c \tag{9}$$

where C is the concentration in the macropores, which varies with time and radial position in the sorbent. The loading on the microparticle surface is described by Langmuir isotherm

$$q=\frac{q_s bC}{1+bC} \tag{10}$$

and the micropore diffusivity is represented by Darken's law:

$$D_c=D_{c0}\frac{d\,\mathrm{In}(C)}{d\,\mathrm{In}(q)} \tag{11}$$

where D_{c0} is the limiting micropore diffusivity at zero adsorbate concentration.

2.3 AD-LDF approximation

The concentration-dependent diffusivity for the mass transfer in micropores, i.e., D_c in Eq. (6), can be replaced by an average diffusivity as an approximation (Garg and Ruthven 1972). With the averaged diffusivity, the LDF model, Eq. (1), can be used to approximate Eq. (6) for the mass transfer in micropores. The average diffusivity is described by

$$\overline{D_c} = \frac{\int_0^{q_{\max}} D_{c0} \frac{d\ln(C)}{d\ln(q)} dq}{\int_0^{q_{\max}} dq} \tag{12}$$

$$\frac{\partial \overline{q}}{\partial t} = \frac{15\overline{D_c}}{r_c^2}(q^* - \overline{q}) \tag{13}$$

Table 1 Properties of sorbents, and parameters of kinetics and equilibrium

Property	Symbol	Units	Value
Sorbent radius	R_p	m	10^{-3}
Crystal radius	r_c	m	10^{-6}
Pellet porosity	ε	–	0.44
Macropore diffusivity (considering tortuosity)	D_p	m^2/s	10^{-5}
Limiting micropore diffusivity at zero loading in crystals	D_{c0}	m^2/s	2×10^{-14}
Saturation loading in crystals	q_s	mol/m^3	771.3
Langmuirian gas–solid interaction parameter	b	m^3/mol	0.5

where q_{max} is the maximum loading in the micropores of the sorbents during the sorption process. The equilibrium loading on the crystal surface (q^*), which is the function of time and radial position of the pellet (R), is determined according to Eq. (10) with the corresponding concentration in macropores [$C(t,R)$].

2.4 CDD-LDF approximation

In the microparticle, the volume-average loading and its time derivative are

$$\overline{q} = \frac{1}{\frac{4}{3}\pi r_c^3} \int_0^{r_c} q(r,t) 4\pi r^2 dr = \frac{3}{r_c^3} \int_0^{r_c} q(r,t) r^2 dr \tag{14}$$

$$\frac{\partial \overline{q}}{\partial t} = \frac{3}{r_c^3} \int_0^{r_c} \frac{\partial q}{\partial t} r^2 dr \tag{15}$$

Combining Eqs. (6), (11) and (15), and replacing q with $\overline{q}$ in Eq. (11) as a compromise between satisfying the parabolic concentration profile and best approximating the

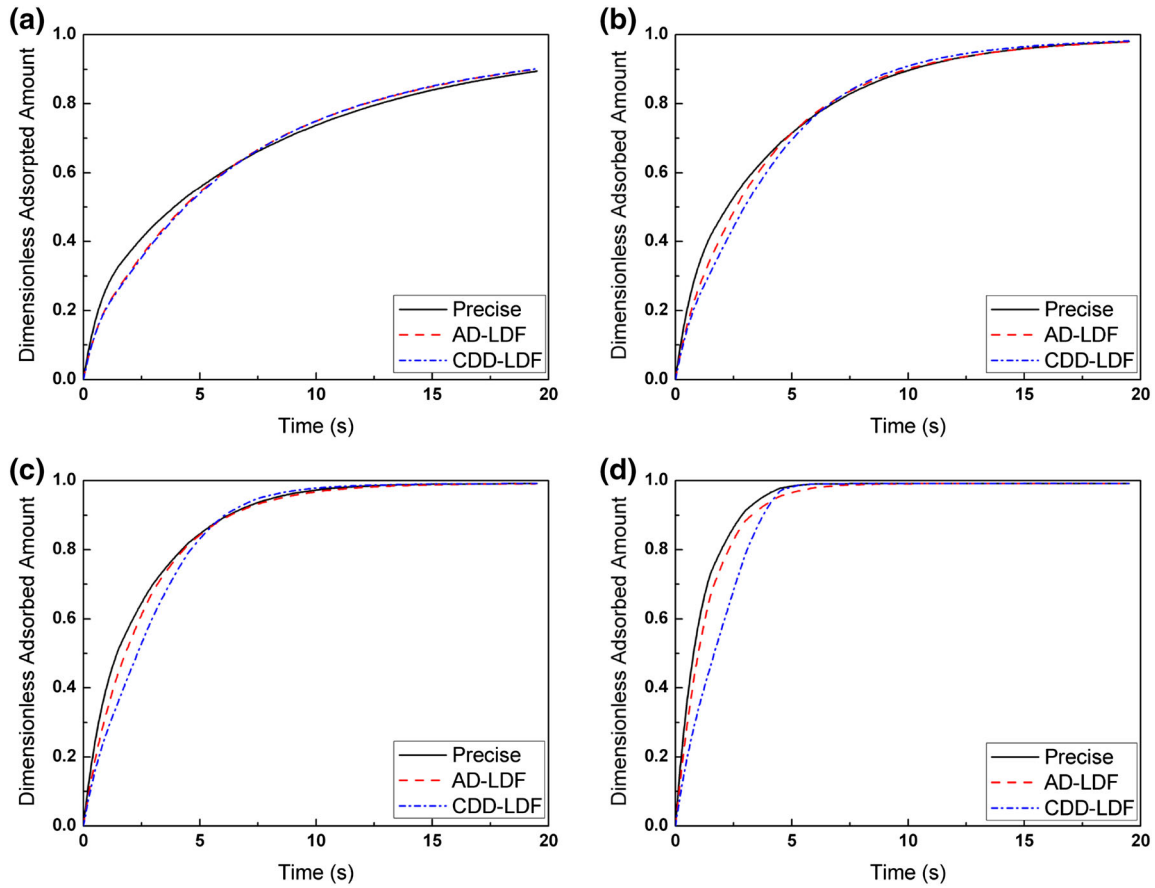

Fig. 1 Uptake curves for the step adsorption perturbation (Eq. 24). Dimensionless maximum loading (q_{max}/q_s) in crystals is **a** 0.1, **b** 0.5, **c** 0.7 and **d** 0.9 during the sorption process

precise model, the time derivative of the volume-average loading becomes

$$\frac{\partial \overline{q}}{\partial t}=\frac{3}{r_c^3}\int_0^{r_c}\frac{\partial}{\partial r}\left(r^2 D_{c0}\frac{\partial \ln(C)}{\partial \ln(\overline{q})}\frac{\partial q}{\partial r}\right)dr=\frac{3}{r_c^3}D_{c0}\frac{\partial \ln(C)}{\partial \ln(\overline{q})}\frac{\partial q}{\partial r}\bigg|_{r=r_c} \tag{16}$$

In the microparticle, a parabolic loading profile is assumed (Liaw et al. 1979), i.e.,

$$q(t,r)=A(t)+B(t)r^2 \tag{17}$$

where A(t) and $B(t)$ are functions of time, which can be determined from the two boundary conditions, i.e., Eqs. (7) and (8).

$$A(t)=q(t,r_c)-\frac{5}{2}[q(t,r_c)-\overline{q}] \tag{18}$$

$$B(t)=\frac{5}{2r_c^2}[q(t,r_c)-\overline{q}] \tag{19}$$

Substituting Eqs. (18) and (19) into Eq. (17), we obtain

$$q(t,r)=q(t,r_c)-\frac{5}{2}[q(t,r_c)-\overline{q}]+\frac{5}{2r_c^2}[q(t,r_c)-\overline{q}]r^2 \tag{20}$$

Then the radial derivative of the loading in the microparticles is

$$\frac{\partial q}{\partial r}\bigg|_{r=r_c}=\frac{5}{r_c}[q(t,r_c)-\overline{q}] \tag{21}$$

Finally, substituting Eq. (21) into Eq. (16), we have the CDD-LDF approximation,

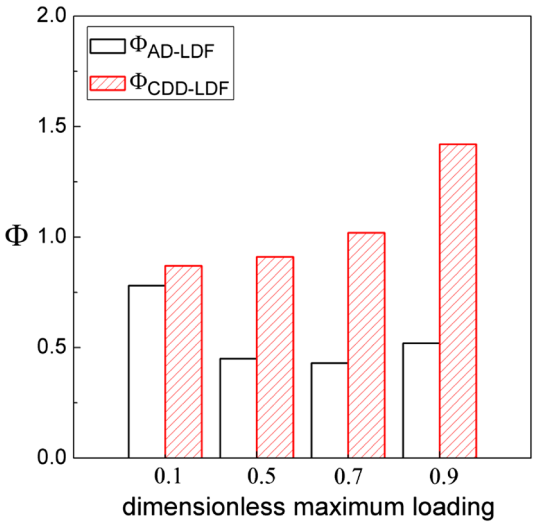

Fig. 2 Dimensionless absolute deviations under the step adsorption perturbation. $\Phi_{AD\text{-}LDF}$ and $\Phi_{CDD\text{-}LDF}$ are described by Eqs. (27) and (28), respectively

$$\frac{\partial \overline{q}}{\partial t}=\frac{15}{r_c^2}D_{c0}\frac{\partial\, In(C)}{\partial\, In(\overline{q})}(q^*-\overline{q}) \tag{22}$$

where $dln(C)/dln(\overline{q})$ is determined by Eq. (10). Comparing the AD-LDF (Eq. 13) with the CDD-LDF (Eq. 22) we can see that they have the same form but different definitions of diffusivity. The equilibrium loading on the crystal surface (q^*) is identical to the one in Eq. (13), ensuring that AD-LDF and CDD-LDF share the same boundary condition on the crystal surface. The deduced Eq. (22) in this paper is identical to the one directly used in the literature of Grande and Rodrigues (2005) as well as Khalighi et al. (2012)

2.5 Comparison between AD-LDF and CDD-LDF

The performances of AD-LDF and CDD-LDF are systematically studied under two types of perturbations imposed at the particle surface, i.e., step change and sinusoidal wave perturbations. The step change perturbations reflect the condition at the inlet of the adsorption column, while the sinusoidal wave perturbation corresponds to a smooth variation of concentrations inside the adsorption column (Cruz et al. 2006).

The step change perturbations are described by

$$C_b=C_h\ (adsorption) \tag{23}$$

$$C_b=0\ (desorption) \tag{24}$$

and the sinusoidal wave perturbation is represented by

$$C_b=\begin{cases}C_h\dfrac{\left(\sin\left(\dfrac{2\pi\Delta t_a}{\Delta T_a}-\dfrac{1}{2}\pi\right)+1\right)}{2} & (adsorption\,period)\\ C_h\dfrac{\left(\sin\left(\dfrac{2\pi\Delta t_d}{\Delta T_b}-\dfrac{1}{2}\pi\right)+1\right)}{2} & (desorption\,period)\end{cases} \tag{25}$$

where Δt_a and Δt_d are adsorption time and desorption time, ΔT_a and ΔT_d are the perturbation periods for adsorption and desorption. C_h is the upper limit, while zero is the lower limit.

The dimensionless adsorbed amount of adsorbate (θ) is defined by

$$\theta=\frac{\int_0^{R_p}\overline{q(R,t)}4\pi R^2 dR}{q_{\max}\frac{4}{3}\pi R_p^3} \tag{26}$$

where $\overline{q(R,t)}$, the volume-average microparticle loading calculated from Eqs. (13) or (22), is a function of time and radial position in the sorbent.

For a reasonable evaluation of the performances of AD-LDF and CDD-LDF, the dimensionless absolute deviations between the approximations and precise solution are used:

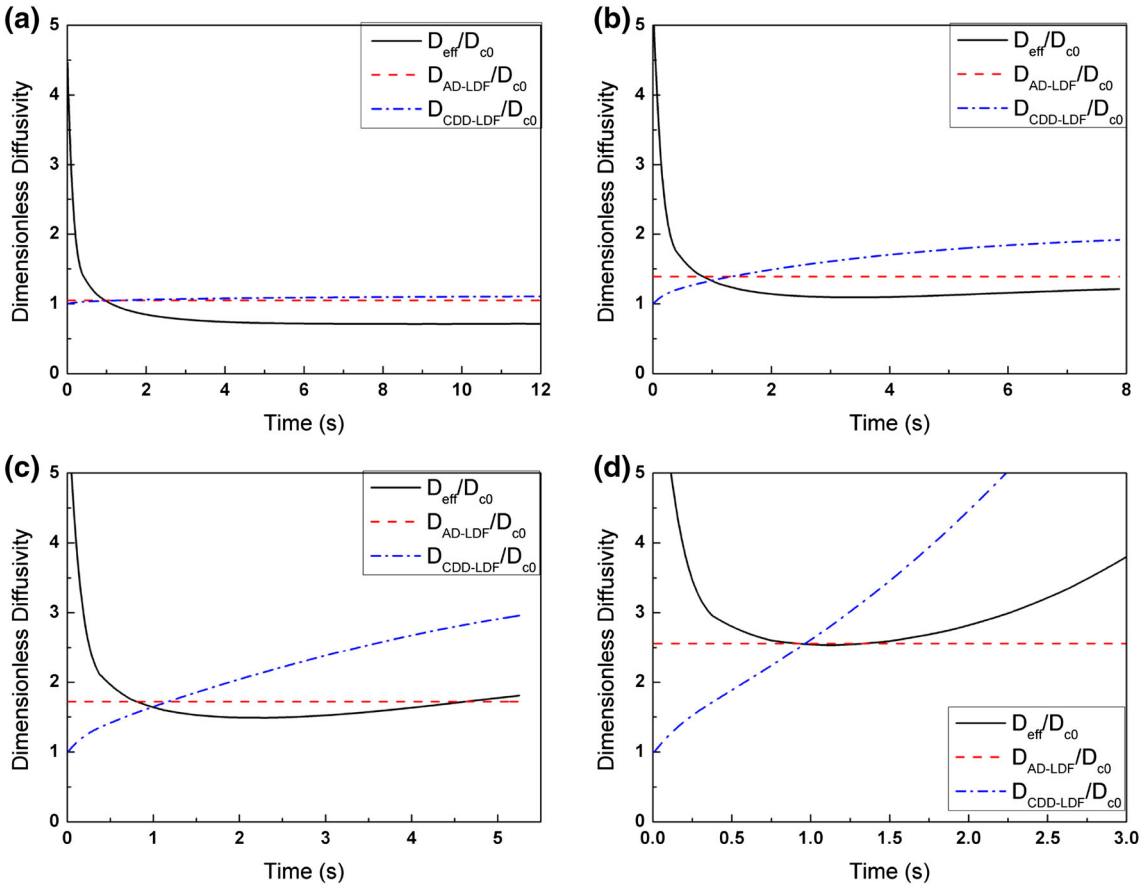

Fig. 3 Dimensionless diffusivities (D_{eff}/D_{c0}, $D_{AD\text{-}LDF}/D_{c0}$ and $D_{CDD\text{-}LDF}/D_{c0}$) for the step adsorption perturbation. Dimensionless maximum loading in crystals is **a** 0.1, **b** 0.5, **c** 0.7 and **d** 0.9 during the sorption process

$$\phi_{AD-LDF} = \sum \left|\theta_{AD-LDF} - \theta_{precise}\right| \tag{27}$$

$$\phi_{CDD-LDF} = \sum \left|\theta_{CDD-LDF} - \theta_{precise}\right| \tag{28}$$

3 Results and discussion

To compare the performance of AD-LDF and CDD-LDF under different perturbations, they are used to simulate the diffusion of 2-methylpentane (2-MP) in the bidisperse silicalite sorbent, with the solutions of precise model as a standard. Table 1 summarizes the parameters for simulation, which are adopted from Jolimaitre et al. (2002).

3.1 Step adsorption perturbation

Figure 1 shows the uptake curves of the precise model, the AD-LDF and the CDD-LDF under step adsorption perturbation, and Fig. 2 shows the dimensionless deviations of the AD-LDF and the CDD-LDF from the precise model. The time-dependent adsorbed amount calculated by the AD-LDF is relatively closer to the precise solution (as seen in Figs. 1 and 2), indicating that the AD-LDF is the more favorable approximation under the step adsorption perturbation.

For a easy understanding of the different levels of the consistency of the two approximations with the precise model, we use a sorption rate equation of the same form of the AD-LDF and the CDD-LDF to fit the precise model, i.e.,

$$\frac{\partial \overline{q}}{\partial t} = \frac{15 D_{eff}}{r_c^2}(q^* - \overline{q}) \tag{29}$$

where D_{eff} is the time dependent effective diffusivity determined by fitting the precise solution. Then, the different levels of the consistency of the two approximations with the precise model can be finally attributed to the different diffusivities.

The effective diffusivity can be obtained in analytical form (Hsuen 2000; Carta 1993) when it is assumed concentration-independent. However, it is concentration-dependent in this work and can be calculated numerically as follows,

$$D_{eff}(t_n) = r_c^2 \frac{[\overline{q}(t_{n+1}) - \overline{q}(t_n)]/(t_{n+1} - t_n)}{15[q^* - \overline{q}(t_n)]} \quad n = 1, 2, 3\ldots \tag{30}$$

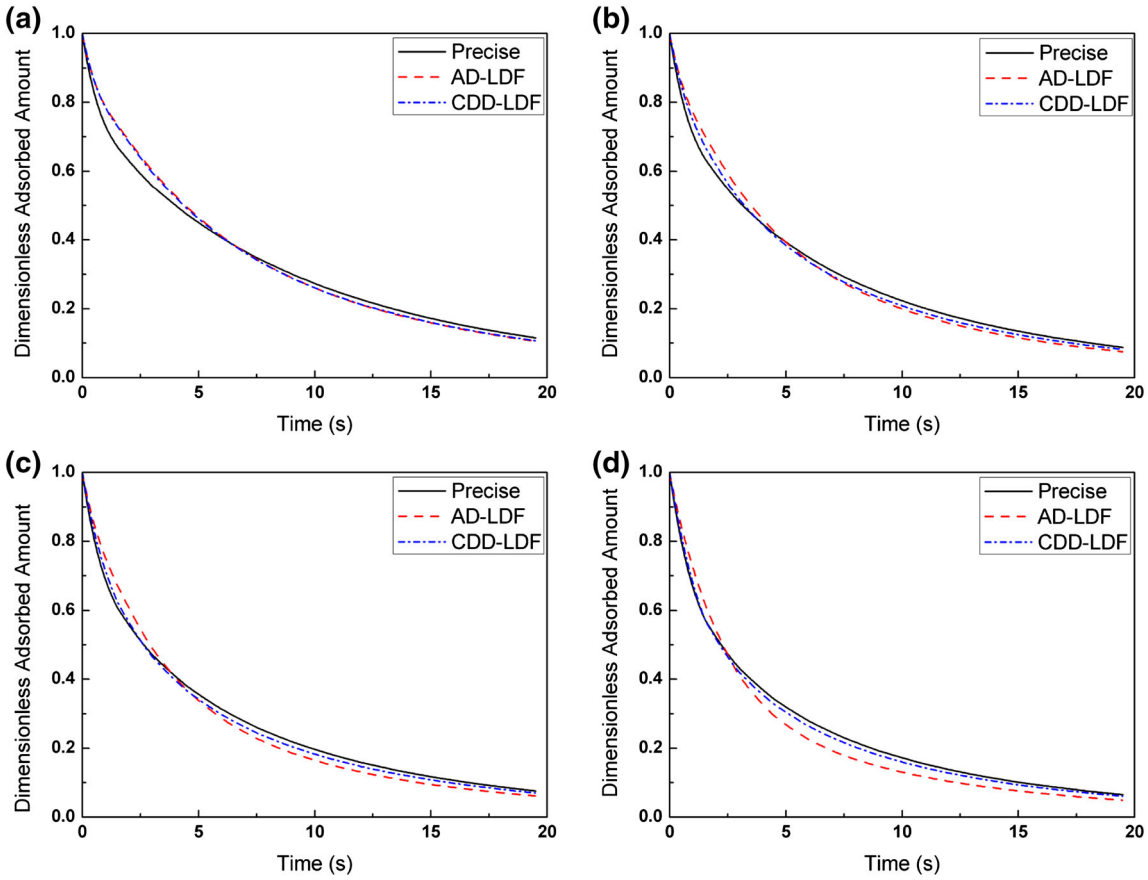

Fig. 4 Uptake curves for the step desorption perturbation (Eq. 25). Dimensionless maximum loading in crystals is **a** 0.1, **b** 0.5, **c** 0.7 and **d** 0.9 during the sorption process

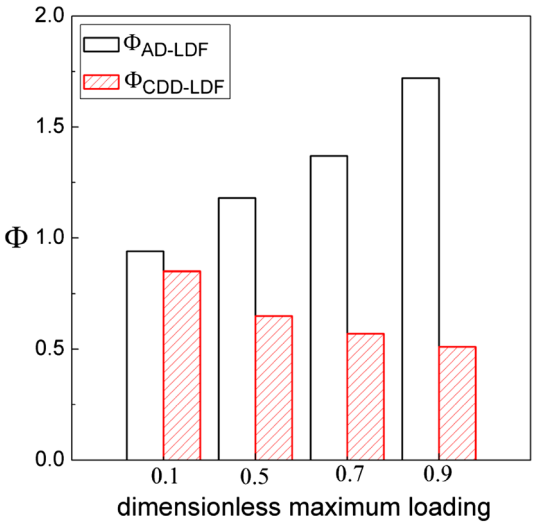

Fig. 5 Dimensionless absolute deviations under the step desorption perturbation. $\Phi_{AD\text{-}LDF}$ and $\Phi_{CDD\text{-}LDF}$ are described by Eqs. (27) and (28), respectively

where $\overline{q}(t_n)$ is obtained by numerically solving the precise model at the 'nth' time point. Figure 3 presents the D_{eff}, $D_{AD\text{-}LDF}$ and $D_{CDD\text{-}LDF}$ with different dimensionless maximum loadings (0.1, 0.5, 0.7 and 0.9) under the step adsorption perturbation. Comparing with $D_{CDD\text{-}LDF}$, $D_{AD\text{-}LDF}$ is closer to D_{eff}, which is responsible for the better performance of the AD-LDF approximation.

3.2 Step desorption perturbation

The precise model, AD-LDF and CDD-LDF are compared under the step desorption perturbation with different dimensionless maximum loadings, and the results are shown in Figs. 4 and 5. The time-dependent adsorbed amount calculated by CDD-LDF is much closer to the precise solution (as seen in Fig. 4) and $\Phi_{CDD\text{-}LDF}$ is smaller than the corresponding $\Phi_{AD\text{-}LDF}$ (as seen in Fig. 5), especially at high adsorbate concentrations, which means that CDD-LDF is the more favorable approximation under the step desorption perturbation.

For the step desorption perturbation, the time dependent D_{eff} could also be obtained in the numerical way according to Eq. (30). However, when the desorption time is long, the D_{eff} cannot be accurately calculated with the numerical method due to the truncation error and roundoff error, and the D_{eff} would be around $2/3D_{C0}$ according to the work of

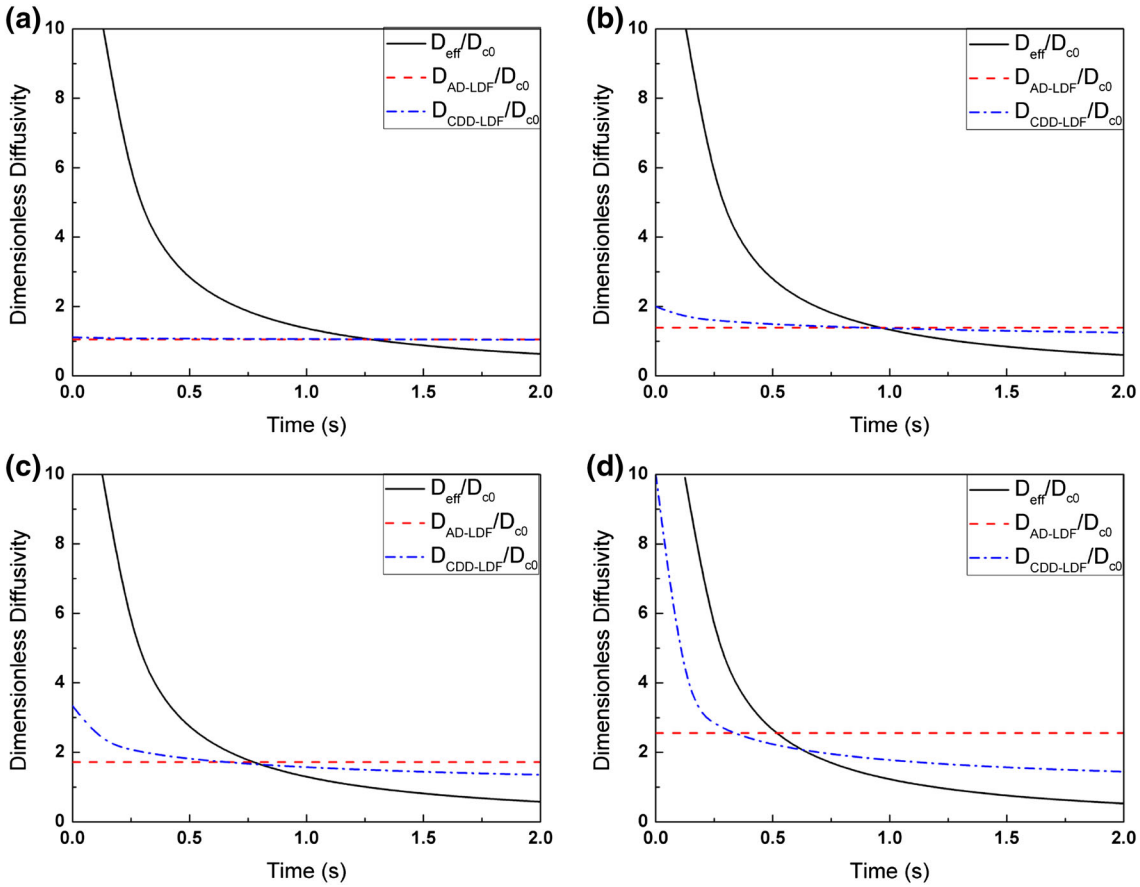

Fig. 6 Dimensionless diffusivities (D_{eff}/D_{c0}, $D_{AD\text{-}LDF}/D_{c0}$ and $D_{CDD\text{-}LDF}/D_{c0}$) for the step desorption perturbation. Dimensionless maximum loading in crystals is **a** 0.1, **b** 0.5, **c** 0.7 and **d** 0.9 during the sorption process

Hsuen (2000). The D_{eff} presented in Fig. 6 is determined within 2 s as the data is reliable and sufficient to explain the results in Fig. 4. Comparing with $D_{AD\text{-}LDF}$, $D_{CDD\text{-}LDF}$ is closer to D_{eff}, which is responsible for the better consistency level the CDD-LDF with the precise model.

3.3 Sinusoidal wave perturbation

The precise model, AD-LDF and CDD-LDF are further evaluated under the sinusoidal wave perturbation with different dimensionless maximum loadings. The results are presented in Figs. 7 and 8.

The time-dependent adsorbed amount of AD-LDF is relatively closer to the precise solution during the adsorption period, while the time-dependent adsorbed amount calculated by CDD-LDF is relatively closer during desorption period. All these results coincide with the ones under the step change perturbations, and can also be explained in the same way, which are presented in part 3.1 and 3.2.

In Fig. 8, $\Phi_{CDD\text{-}LDF}$ is slightly higher than $\Phi_{AD\text{-}LDF}$ when the dimensionless maximum loading is small, i.e., 0.1 and 0.5, and is however much smaller than $\Phi_{AD\text{-}LDF}$ when it is large, i.e., 0.7 and 0.9. Generally, the CDD-LDF is a better approximation under the sinusoidal wave perturbation, especially at high loading in sorbent.

3.4 Validation with experiments

To further validate the AD-LDF and CDD-LDF approximations, they are used to simulate a sorption process without macropores and compare with traditional LDF approximation and experimental data available from literature (Garg and Ruthven 1972; Ruthven 2004). The results are shown in Figs. 9 and 10. The same conclusions can be made that AD-LDF performs better in adsorption stage,

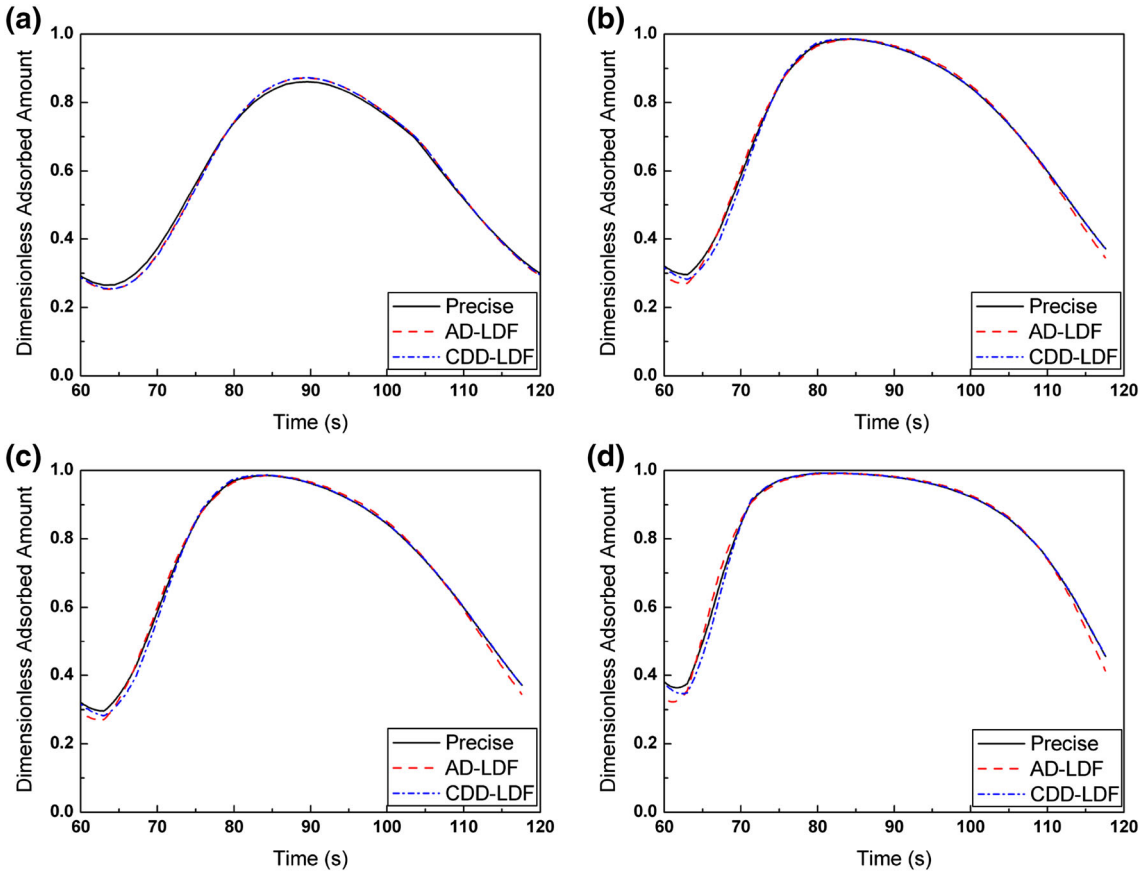

Fig. 7 Uptake curves under sinusoidal wave perturbation (Eq. 26). Dimensionless maximum loading in crystals is **a** 0.1, **b** 0.5, **c** 0.7 and **d** 0.9 during the sorption process

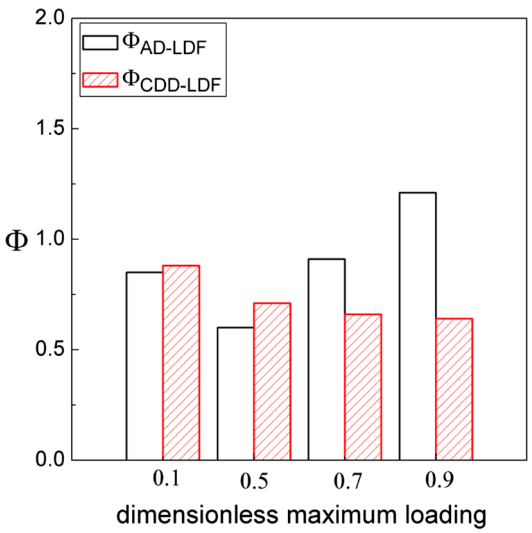

Fig. 8 Dimensionless absolute deviations under sinusoidal wave perturbation. $\Phi_{AD\text{-}LDF}$ and $\Phi_{CDD\text{-}LDF}$ are described by Eqs. (27) and (28), respectively

while the CDD-LDF does better in desorption stage. In general, both are better approximations than traditional LDF. Even better results can be obtained when AD-LDF and CDD-LDF are used alternatively at different stages in sorption processes.

4 Conclusions

In this work we systematically evaluate two LDF based approximations, i.e., the AD-LDF and the CDD-LDF, for concentration-dependent micropore diffusion in bidisperse sorbents. AD-LDF has a better consistency with the precise model under step adsorption perturbation. However, the CDD-LDF is more favorable when the process is subject to the step desorption perturbation. When it is under sinusoidal wave perturbation, the CDD-LDF performs better than the AD-LDF, especially at high adsorbate concentrations. We attribute these results to the difference between the diffusivities of the two approximations and the effective diffusivities of the precise model. In general, both approximations are better than traditional LDF, and even better performance can be expected when AD-LDF and CDD-LDF are used alternatively at different stages in sorption processes.

LDF based approximations perform reasonably well in the time region where the sorption equilibrium is about to be

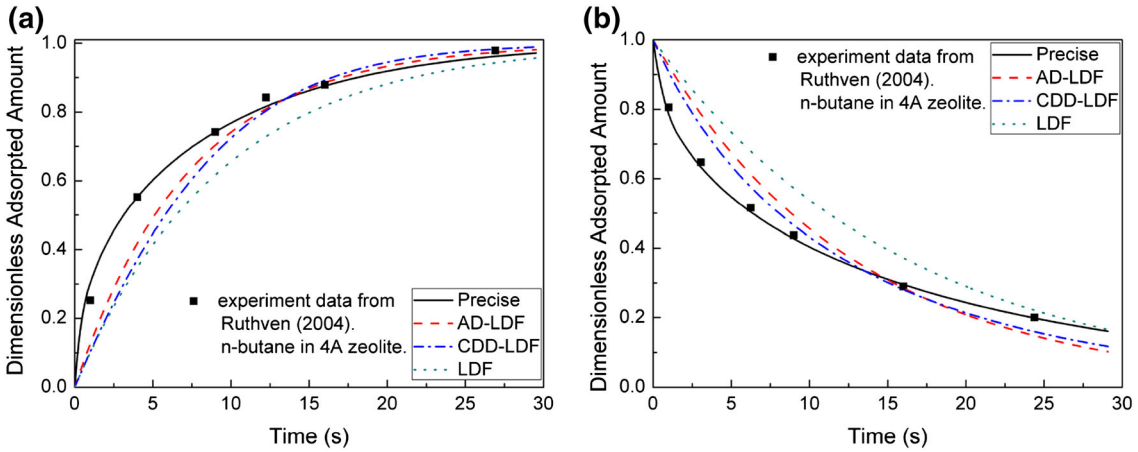

Fig. 9 Comparison between the experimental data from Ruthven (2004) and uptake curves of precise model, AD-LDF, CDD-LDF and traditional LDF under **a** step adsorption perturbation and **b** step desorption perturbation. The dimensionless maximum loading is 0.39

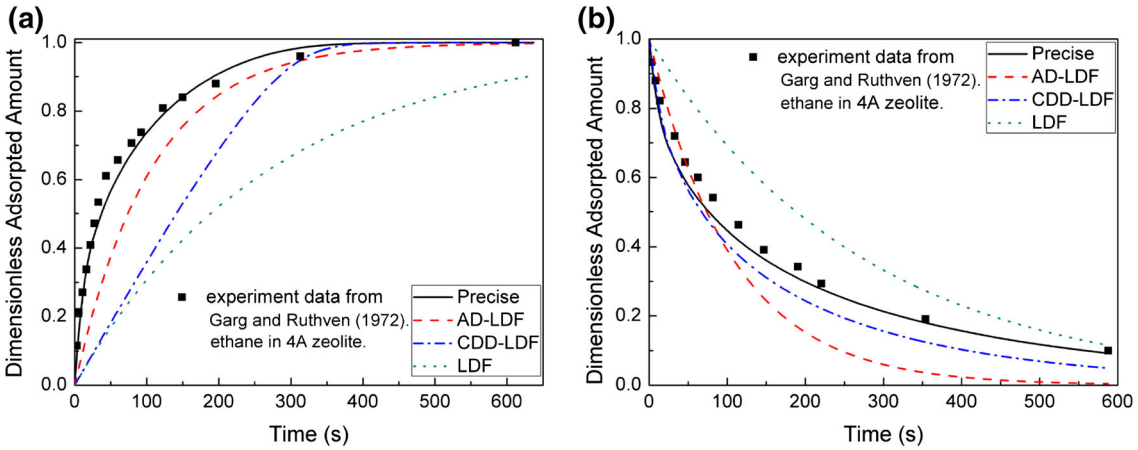

Fig. 10 Comparison between the experimental data from Garg and Ruthven (1972) and uptake curves of precise model, AD-LDF, CDD-LDF and traditional LDF under **a** step adsorption perturbation and **b** step desorption perturbation. The dimensionless maximum loading is 0.9

reached, which indicates the parabolic approximation is accurate in that region. However, according to the precise model, the uptake rate is infinite at zero time, which is hard to be replicated by any LDF based models. This leads to a strong variation in the apparent transport coefficient at the beginning of adsorption or desorption. Therefore, in some modeling situations where the adsorption–desorption cycle period is very short, the deviations between the real uptake curve and the ones calculated by LDF based approximations can be significant.

Acknowledgments The authors are grateful for the financial support of the National Basic Research Program of China (2012CB720501), the National Natural Science Foundation of China (U1162112), and the New Century Excellent Talents in University of the Chinese Department of Education (NCET-11-0644).

References

Azevedo, D.C.S., Rodrigues, A.E.: Bilinear driving force approximation in the modeling of a simulated moving bed using bidisperse adsorbents. Ind. Eng. Chem. Res. **38**(9), 3519–3529 (1999a)

Azevedo, D.C.S., Rodrigues, A.E.: Design of a simulated moving bed in the presence of mass-transfer resistances. AIChE J. **45**(5), 956–966 (1999b)

Botte, G.G., Zhang, R., Ritter, J.A.: New approximate model for nonlinear adsorption and concentration dependent surface diffusion in a single particle. Adsorption **5**, 373–380 (1999)

Carta, G.: The linear driving force approximation for cyclic mass transfer in spherical particles. Chem. Eng. Sci. **48**(3), 622–625 (1993)

Cruz, P., Magalhaes, F.D., Mendes, A.: Generalized linear driving force approximation for adsorption of multicomponent mixtures. Chem. Eng. Sci. **61**, 3519–3531 (2006)

Do, D.D.: Hierarchy of rate models for adsorption and desorption in bidisperse structured sorbents. Chem. Eng. Sci. **45**(5), 1373–1381 (1990)

Do, D.D.: Adsorption analysis: Equilibria and kinetics. Imperial College Press, London (1998)

Do, D.D., Rice, R.G.: Revisiting approximate solutions for batch adsorbers: explicit half time. AIChE J. **41**(2), 426–429 (1995)

Farooq, S., Rathor, M.N., Hidajat, K.: A predictive model for a kinetically controlled pressure swing adsorption separation process. Chem. Eng. Sci. **48**(24), 4129–4141 (1993)

Farooq, S., Ruthven, D.M.: Numerical simulation of a kinetically controlled pressure swing adsorption bulk separation process

based on a diffusion model. Chem. Eng. Sci. **46**(9), 2213–2224 (1991)

Garg, D.R., Ruthven, D.M.: The effect of the concentration dependence of diffusivity on zeolitic sorption curves. Chem. Eng. Sci. **27**, 417–423 (1972)

Glueckauf, E., Coates, J. I.: The influence of incomplete equilibrium on the front boundary of chromatograms and the effectiveness of separation. J. Chem. Soc. 1315–1321 (1947)

Goto, M., Hirose, T.: Approximate rate equation for intraparticle diffusion with or without reaction. Chem. Eng. Sci. **48**(10), 1912–1915 (1993)

Goto, M., Smith, J.M., McCoy, B.J.: Parabolic profile approximation (linear driving-force model) for chemical reactions. Chem. Eng. Sci. **45**(2), 443–448 (1990)

Grande, C.A., Rodrigues, A.E.: Adsorption of binary mixtures of propane-propylene in carbon molecular sieve 4A. Ind. Eng. Chem. Res. **43**(25), 8057–8065 (2004)

Grande, C.A., Rodrigues, A.E.: Propane/propylene separation by pressure swing adsorption using zeolite 4A. Ind. Eng. Chem. Res. **44**(23), 8815–8829 (2005)

Hsuen, H.K.: An improved linear driving force approximation for intraparticle adsorption. Chem. Eng. Sci. **55**(17), 3475–3480 (2000)

Hu, X., Do, D.D.: Contribution of concentration-dependent surface diffusion in ternary adsorption kinetics of ethane, propane and n-butane in activated carbon. Adsorption **2**, 217–225 (1996)

Jobic, H., Kärger, J., Krause, C., Brandani, S., Gunadi, A., Methivier, A., Ruthven, D.M.: Diffusivities of n-alkanes in 5A zeolite measured by neutron spin echo, pulsed-field gradient, NMR, and zero length column techniques. Adsorption **11**, 403–407 (2005)

Jolimaitre, E., Ragil, K., Tayakout-Fayolle, M., Jallut, C.: Separation of mono-and dibranched hydrocarbons on silicalite. AIChE J. **48**(9), 1927–1937 (2002)

Jolimaitre, E., Tayakout-Fayolle, M., Jallut, C., Ragil, K.: Determination of mass transfer and thermodynamic properties of branched paraffins in silicalite by inverse chromatography. Ind. Eng. Chem. Res. **40**(3), 914–926 (2001)

Khalighi, M., Farooq, S., Karimi, I.A.: Nonisothermal pore diffusion model for a kinetically controlled pressure swing adsorption process. Ind. Eng. Chem. Res. **51**, 10659–10670 (2012)

Kärger, J., Ruthven, D.M.: Diffusion in zeolites and other microporous solids. Wiley, New York (1992)

Krishna, R., Baur, R.: Modelling issues in zeolite based separation processes. Sep. Purif. Technol. **33**(3), 213–254 (2003)

Li, Z., Yang, R.T.: Concentration profile for linear driving force model for diffusion in a particle. AIChE J. **45**(1), 196–200 (1999)

Liu, Z., Wang, L., Kong, X.M., Li, P., Yu, J.G., Rodrigues, A.E.: Onsite CO_2 capture from flue gas by an adsorption process in a coal-fired power plant. Ind. Eng. Chem. Res. **51**(21), 7355–7363 (2012)

Lai, C.C., Tan, C.S.: Approximate models for nonlinear adsorption in a packed-bed adsorber. AIChE J. **37**(3), 461–465 (1991)

Lettat, K., Jolimaitre, E., Tayakout, M., Tondeur, D.: Liquid phase diffusion of branched alkanes in silicalite. AIChE J. **57**(2), 319–332 (2011)

Liaw, C.H., Wang, J.S.P., Greenkorn, R.A., Chao, K.C.: Kinetics of fixed bed adsorption: a new solution. AIChE J. **25**(2), 376–381 (1979)

Ruckenstein, E., Vaidyanathan, A.S., Youngquist, G.R.: Sorption by solids with bidisperse pore structures. Chem. Eng. Sci. **26**, 1305–1318 (1971)

Ruthven, D.M.: Fundamentals of adsorption equilibrium and kinetics in microporous solids. Mol. Sieves **7**, 1–43 (2008)

Ruthven, D.M.: Sorption kinetics for diffusion-controlled systems with a strongly concentration-dependent diffusivity. Chem. Eng. Sci. **59**(21), 4531–4545 (2004)

Ruthven, D.M., Brandani, S., Eic, M.: Measurement of diffusion in microporous solids by macroscopic methods. Mol. Sieves **7**, 45–84 (2008)

Ruthven, D.M., Loughlin, K.F.: The diffusional resistance of molecular sieve pellets. Can. J. Chem. Eng. **50**, 550–552 (1972)

Skoulidas, A.I., Sholl, D.S.: Direct tests of the darken approximation for molecular diffusion in zeolites using equilibrium molecular dynamics. J. Phys. Chem. B **105**(16), 3151–3154 (2001)

Solsvik, S., Jakobsen, H.A.: Modeling of multicomponent mass diffusion in porous spherical pellets: application to steam methane reforming and methanol synthesis. Chem. Eng. Sci. **66**(9), 1986–2000 (2011)

Xiu, G.: Modeling breakthrough curves in a fixed bed of activated carbon fiber—exact solution and parabolic approximation. Chem. Eng. Sci. **51**(16), 4039–4041 (1996)

Xiu, G., Nitta, T., Li, P., Jin, G.: Breakthrough curves for fixed-bed adsorbers: quasi-lognormal distribution approximation. AIChE J. **43**(4), 979–985 (1997)

Yao, C., Tien, C.: Approximations of uptake rate of spherical adsorbent pellets and their application to batch adsorption calculations. Chem. Eng. Sci. **48**(1), 187–198 (1993)

Yao, C., Chi, T.: New models for evaluating the adsorption rate of an adsorbent. Chin. J. Chem. Eng. **6**(1), 1–11 (1998)

Zhang, R., Ritter, J.A.: New approximate model for nonlinear adsorption and diffusion in a single particle. Chem. Eng. Sci. **52**(18), 3161–3172 (1997)